Progressive Cavitating Leukoencephalopathy: A Novel Childhood Disease

SakkuBai Naidu, MD,[1] Genila Bibat, MD,[1] Doris Lin, MD,[2] Peter Burger, MD,[3] Peter Barker, PhD,[2] Sergio Rosemberg, MD,[4] Nancy Braverman, MD,[5] Hugo Arroyo, MD,[6] Michael Dowling, MD, PhD,[7] Ada Hamosh, MD,[5] Virginia Kimonis, MD,[8] Carol Blank, MD,[9] Agata Fiumara, MD,[10] Sergio Facchini, MD,[11] Bhim Singhal, MD,[12] Hugo Moser, MD,[1] Richard Kelley, MD, PhD,[1] and Salvatore DiMauro, MD[13]

We report 19 patients with a previously undelineated neurodegenerative syndrome characterized by episodic acute onset of irritability or neurological deficits between 2 months and 3.5 years of age, followed by steady or intermittent clinical deterioration. Seven children died between 11 months and 14 years of age. Cranial magnetic resonance imaging (MRI) shows patchy leukoencephalopathy with cavities, and vascular permeability, in actively affected regions. Early lesions affect corpus callosum and centrum semiovale, with or without cerebellar or cord involvement. After repeated episodes, areas of tissue loss coalesce with older lesions to become larger cystic regions in brain or spinal cord. Diffuse spasticity, dementia, vegetative state, or death ensues. Gray matter is spared until late in the course. In some, incomplete clinical or MRI recovery occurs after episodes. The clinical course varies from rapid deterioration to prolonged periods of stability that are unpredictable by clinical or MRI changes. Elevated levels of lactate in brain, blood, and cerebrospinal fluid, abnormal urine organic acids, and changes in muscle respiratory chain enzymes are present but inconsistent, without identifiable mitochondrial DNA mutations or deletions. Pathological studies show severe loss of myelin sparing U-fibers, axonal disruption, and cavitary lesions without inflammation. Familial occurrence and consanguinity suggest autosomal recessive inheritance of this distinct entity.

Ann Neurol 2005;58:929–938

Cystic changes in white matter can be seen in many neurodegenerative disorders, in nonprogressive conditions such as stroke, and in periventricular leukomalacia after neonatal hypoxic ischemia. Large cysts can be identified by neuroimaging studies as in leukoencephalopathy associated with megalencephaly (MLC1) or microcephaly,[1–3] but small vacuolizations are identified histologically as in Canavan's disease.[4] We identified 19 patients from 16 families in whom episodic acute clinical deterioration associated with focally enhancing white matter lesions progressed to multifocal cystic degeneration, without identifiable cause. The lattice-like lesions coalesced, rapidly or after periods of remission, destroying larger areas of white matter. Death occurred between 11 months and 14 years of age. The acute neurological events were occasionally associated with mild infections, but there was no histological evidence of cerebral inflammation. The characteristic clinical course and neuroimaging features distinguish this disorder as a unique entity, and the familial occurrence suggests autosomal recessive inheritance.

Subjects and Methods

Of the 19 patients, 15 were initially evaluated for acute onset of neurological deficits and abnormal magnetic resonance imaging (MRI). Except for Cases 7 and 18 who were born at 27 and 28 weeks' gestation, all had normal prenatal and perinatal histories. Ethnicity included nine Hispanics, six whites, and one each of Indonesian, Lebanese, Hispanic/Irish, and Chinese/Portuguese/Russian. Age at onset varied from 2 months to 3.5 years, and death occurred in seven patients between the ages of 11 months and 14 years. There were

From the [1]Neurogenetics Department, Kennedy Krieger Institute; [2]Department of Radiology; and [3]Department of Pathology, Johns Hopkins Medical Institutions, Baltimore, MD; [4]Department of Pathology, Hospital das Clinicas da Universidade de Sao Paulo, Sao Paulo, Brazil; [5]Institute of Genetic Medicine, Johns Hopkins Medical Institutions, Baltimore, MD; [6]Department of Neurology, Hospital de Pediatria, Buenos Aires, Argentina; [7]Department of Neurology, University of Texas Southwestern Medical Center, Dallas, TX; [8]Department of Genetics, Children's Hospital Boston, Boston, MA; [9]Gettysburg Pediatrics, Gettysburg, PA; [10]Department of Neurology, Clinica Pediatrica, Universita di Catania, Italy; [11]Division of Pediatric Neurology, Baylor College of Medicine, Houston, TX; [12]Bombay Hospital, Institute of Medical Science, Medical Research Center, Mumbai, India; and [13]Department of Neurology, Columbia University, New York, NY.

Received Jul 8, 2005, and in revised form Aug 5. Accepted for publication Aug 26, 2005.

Published online Nov 28, 2005 in Wiley InterScience (www.interscience.wiley.com). DOI: 10.1002/ana.20671

Address correspondence to Dr Naidu, MD, The Kennedy Krieger Institute and the Johns Hopkins Medical Institutions, 707 N. Broadway, 5th Floor Tower, Department of Neurogenetics, Baltimore, MD 21205. E-mail: naidu@kennedykrieger.org

Table 1. Clinical and Laboratory Profile of PCL in Patients 1–9

	Patient/Sex								
Characteristic	1/F (sib 1)	2/M (sib 2)	3/F	4/F	5/M	6/F	7/F (sib 1)	8/M (sib 2)	9/M
Onset (mo)	15	24	36	29	43	17	8	9	15
Prior Sx	−	+	+	+	−	+	+	−	−
Initial Acute Sx	Ataxia, opisth irrit seizure	↓ Balance	Ataxia	↑ Fall, tremor	Dysph dysart ataxia	↑Tone; dysph	Irrit, Vomit, dyston abn eye	Floppy abn eye, seizure	Irrit, limp
Events	4	3	6	7	5	3	1	2	1
Treatment	IgG	Carnitor, CoQ	mt. cocktail; IVIg, steroid DCA	CoQ, DCA, mt. cocktail.	pred, IVIg DCA Interferon	mt. cocktail; gabatril steroid	−	−	mt. cocktail.
Course	Spastic Exp-7 yr	Spastic	Spastic Exp-14 yr	Spastic	Spastic	Spastic	Dyston	Spastic Exp 8 yr	Spastic
UOA	NL	NL	Abn, rpt NL	Abn	Abn	Abn	NL	NL	NL
SAA	?	NL	NL	Abn	Abn	Abn	NL	NL	NL
Lactate									
Serum	↑	↑	NL	↑	NL	NL	NT	NT	NL
CSF	NL	NL	↑, NL	↑	↑	↑	NT	NT	↑
MRS	NT	NL	↑	NT	↑	↑	↑	↑	↑
MRS: other	NT	↑cho, myoino ↓NAA	↓cho, NAA, crea	NT	↑ cho	↑ cho,. ↓NAA crea; glu	NL	NL	NL
Neuropathy	NT	NT	+Axonal/ demyel	+ demyel	—	—	—	—	NT
Muscle Histo	NL	NT	NL	Pleom. mt	Mild Fiber 2 atrophy	NL	NL	NL	Fiber 2 atrophy
Mito Studies	NT	MELAS-NARP-	Partial ↓ I; DNA -	↓1&IV DNA -	NL	NT	NT	NT	↓ I, III & IV; ↑c syn; DNA -

I, III, IV = complex I, III, IV deficiencies; Abn = abnormal; abn eye = abnormal eye movements; bal = balance; cho = choline; c.syn = citrate synthase; consang = consanguinity; cr = creatine; demyel = demyelination; CSF = cerebrospinal fluid; DCA =dichloroacetate; DNA = mitochondrial DNA; dysart = dysarthria; dysph = dysphagia; dyston = dystonia; exp = expired; glu = glutamine; Histo = histology; irrit = irritable; mI = myoinositol; Mito = mitochondrial; MRS = magnetic resonance spectroscopy; mt = mitochondrial; NAA = *N*-acetylaspartic acid; NL = normal; NT = Not Tested; opisth = opisthotonus; pleo = mito pleomorphism; Pl.AA = plasma amino acids; sib = sibling; sx = symptoms; ubiqui = ubiquinone; UOA = urine organic acids.

three sets of familial cases (see Table) and consanguinity in two families. Autopsy was performed in three cases and brain biopsy was performed in one.

Subtle developmental delay before onset of the acute episodes was seen in Patients 2 to 4, 6, 7, 14, and 17 to 19. In some, the acute clinical deteriorations required hospitalization, but they were unrelated to infection, trauma, or other identifiable causes. Tests included plasma and urinary amino acids, urine organic acids, blood lactate, blood chemistry, lysosomal enzymes and peroxisomal studies, muscle biopsy for morphology and mitochondrial (mt) analyses, electroencephalogram (EEG), and electromyogram (EMG)/nerve conduction velocity (NCV).

Treatment

Acute management consisted of morphine drips to treat screaming spells, irritability, and posturing that were considered to be pain related. Others included steroids, intravenous immunoglobulin (IVIG), or both in Patients 1, 5, 6, 12, 15, 17 during acute phases, Patients 3, 4, 5 and 17 received dichloroacetate (DCA), Patients 3, 4, 6, 9, and 19 received mt cocktail, and Patient 12 received acyclovir.

Magnetic Resonance Imaging

Thirty-three MRIs were available for study. Studies of the brain typically included sagittal T1-weighted spin-echo (350–500/10–15/1 TR/TE/NEX), axial dual-echo (3,500/119 and 17), and postcontrast axial and coronal T1-weighted spin-echo images. More recent studies included sagittal T1-weighted spin-echo (350–600/7–15), axial fluid attenuated inversion recovery (8,000/80), diffusion-weighted echo planar imaging (9,983, 118, b = 0, and 1,000), and postcontrast axial and coronal T1-weighted spin-echo sequences. Contrast was administered once in Patients 18 and

Table 2. Clinical and Laboratory Profile of PCL in Patients 10–19

	Patient/Sex									
Characteristics	10/M +	11/F	12/F	13/M (sib 1) +	14/F (sib 2) +	15/M	16/F	17/F	18/F	19/M
Onset (mo)	12	10	20	2	6	24	9	22	20	9
Prior Sx	−	−	−	−	+	−	−	+	+	+
Initial Acute Sx	No walk	Legs weak	Coma	Poor suck	Irrit; weak	↓ Bal	Irrit; limp	Irrit; opisth	Toe−walk	Fever vomit
Events	3	1	2	3	1	1	3	6	1	Many
Treatment	−	−	γ Glob; Acyclovir; Steroid	−	−	Steroid	Na Benz	Dexam, DCA; IVIg	-	Ubiqui B1, B2
Course	Spastic	Spastic	Spastic Exp 4 yr	spastic Exp 1 yr	Exp. 1.2 yr	Spastic	Spastic	Exp. 3.5 yr	Spastic	Spastic
UOA	NT	NL	NL	NT	NL	NL	NT	NL	NL	NT
SAA	NL	NL	NL	NT	NL	NL	Abn	NL	NL	NL
Lactate										
Serum	NT	NT	NT NT	NT	↑	↑	NL	↑	NT	↑
CSF	NT	NT	NT	NT	NT	NT	NL	↑	↑	↑
MRS	NT	NT		NT	NL	NT	↑	NT	NT	↑
MRS: other	NT	NT	NT	NT	NL	NT	NL	NT	NT	NL
Neuropathy	NT	NT	NT	NL	NT	NT	NT	-	-	NT
Muscle Histo	NT	NT	NT	Non-specfic atrophy	NT	NT	NL	Fiber 2 atrophy	NL	NL
Mito Studies	NT	Melas-	NT	NT	NT	NT	NL	DNA-	NL	NL

I, III, IV = complex I, III, IV deficiencies; Abn = abnormal; abn eye = abnormal eye movements; bal = balance; cho = choline; c.syn = citrate synthase; consang = consanguinity; cr = creatine; demyel = demyelination; CSF = cerebrospinal fluid; DCA =dichloroacetate;DNA = mitochondrial DNA; dysart = dysarthria; dysph = dysphagia; dyston = dystonia; exp = expired; glu = glutamine; Histo = histology; irrit = irritable; mI = myoinositol; Mito = mitochondrial; MRS = magnetic resonance spectroscopy; mt = mitochondrial; NAA = *N*-acetylaspartic acid; NL = normal; NT = Not Tested; opisth = opisthotonus; pleo = mito pleomorphism; Pl.AA = plasma amino acids; sib = sibling; sx = symptoms; ubiqui = ubiquinone; UOA = urine organic acids.

11, twice in Patients 3 and 9, three times in Patient 6, and five times in Patient 5. Three patients also had MRI of the entire spine that included sagittal and axial T1-weighted spin-echo (500/9.8) and T2-weighted fast spin-echo (3,750–5,000/100–120) images.

Magnetic Resonance Spectroscopy

In three patients, proton magnetic resonance spectroscopy (MRS) imaging (MRSI) was performed on a 1.5-Tesla General Electric scanner at an echo time of 280 milliseconds using a multislice spin-echo pulse sequence with water and lipid suppression.[5] In seven other patients, single-voxel MRS scans were available from outside institutions, so that MRS results were available in 10 patients totally (Patients 2, 3, 5–9, 14, 16, and 19). In three children (Patients 2, 3, and 6), MRSI data were available from regions of interest placed in abnormal white matter, cerebrospinal fluid (CSF), and gray matter (Fig 1). In the remaining patients, only the presence or absence of lactate, or reduced *N*-acetyl aspartic acid (NAA), choline (Cho), and creatine (Cr), were evaluated within the white matter lesions themselves.

NCV/EMG

NCV/EMG was performed in Patients 3 to 9, 17 and 18.

Muscle Biopsy

As shown in the Table, muscle biopsy was done in Patients 1, 3 to 9, 13, and 16 to 19. Activities of respiratory chain enzymes were measured in Patients 3 to 5, 9, 11, and 16, and mt DNA mutations were screened in Patients 3, 4, 9, 11, and 17.

Results

Clinical and laboratory findings in our 19 patients are enumerated in the Table and summarized below.

Metabolic and Genetic Testing

No electrolyte imbalance or acidosis was detected during the acute crisis. Studies of lysosomal enzymes ex-

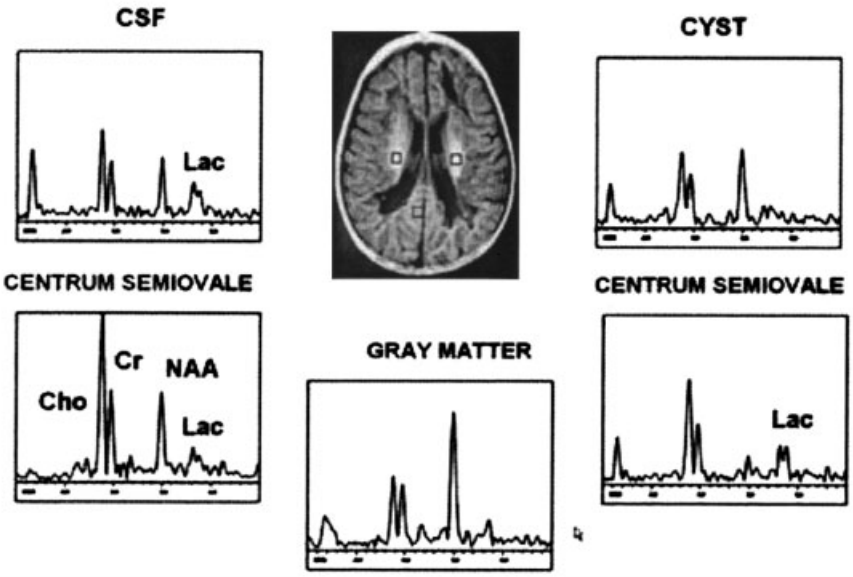

Fig 1. ^{1}H magnetic resonance spectroscopy imaging (MRSI) (TE, 280 milliseconds) in Patient 6, who presented with acute onset of opisthotonus and irritability (postcontrast magnetic resonance images [MRIs] also obtained at the same time are shown in Fig 3E,F). N*-acetyl aspartic acid (NAA) was markedly reduced and lactate was elevated throughout the affected white matter (ie, frontal and posterior periventricular white matter and centrum semiovale bilaterally). In the cystic white matter lesions, the concentration of all metabolites was significantly reduced, whereas in the solid white matter lesions Cho was normal to mildly elevated. Cho was markedly increased only in the right centrum semiovale. All gray matter regions examined had normal MRSI appearance. Lactate was also detected in the ventricular cerebrospinal fluid (CSF).*

cluded metachromatic leukodystrophy, Krabbe disease, adrenoleukodystrophy, and oligosaccharidosis. Plasma amino acid studies also were normal. Vanishing white matter was excluded by testing for mutations in EIF2B in Patient 7. Intermittent changes in urine organic acids included: increased 3-hydroxyisovaleric acid and lactate in Patient 3; increased fumaric, citric, and aconitic acids in Patient 4; slight increase of 3-hydroxybutyric acid and lactic acid in Patient 5; increased 2-ketoglutarate, fumarate and 2-ethylhydracrylate in Patient 6.

Cerebrospinal Fluid Analyses

CSF for myelin basic protein (MBP) and oligoclonal bands were normal in Patients 4 and 5; in Patient 6, MBP level was initially normal but later increased slightly to 5.4ng/ml (normal level, 0–4ng/ml). The CSF cell count, protein, glucose, and cultures were normal in most but abnormal in Patients 1 and 4. Patient 4 had an immunoglobulin G level that was slightly increased, and viral studies in blood and CSF were negative for Patients 6 and 11.

Electroencephalograms

EEGs showed diffuse slow backgrounds in all patients, without evidence of spike activity in the acute phase or during intervening periods, even in those with clinical seizures.

Magnetic Resonance Spectroscopy

In 9 of 10 cases tested by MRS, lactate level was elevated in the affected structures. In the three patients investigated by MRSI, gray matter spectra were within normal limits, whereas abnormal white matter showed decreased levels of NAA, in addition to increased lactate. White matter Cho levels were variable, with reduced levels of Cho (and also Cr) in the most severely affected regions. However, Patient 6 did have an elevated Cho signal in the centrum semiovale. An example of Patient 6 is shown in Figure 1, who presented with acute onset of opisthotonus and severe irritability. MRS performed 1 month later shows markedly reduced NAA and increased lactate throughout the affected white matter and CSF. In the cystic white matter lesions, all metabolites were reduced in concentration, whereas in the solid white matter there was normal to mild elevation of Cho.

Magnetic Resonance Imaging

The initial MRI of all patients showed a characteristic pattern of cystic changes in the corpus callosum, whereas cysts were more variably present in the affected frontal and parietal deep periventricular white matter (eg, Patient 2 in Fig 2). Patient 5, who was examined five times over 6 months, did not have diffuse involvement, but individual cystic lesions increased in the hemispheric white matter and corpus callosum during this short pe-

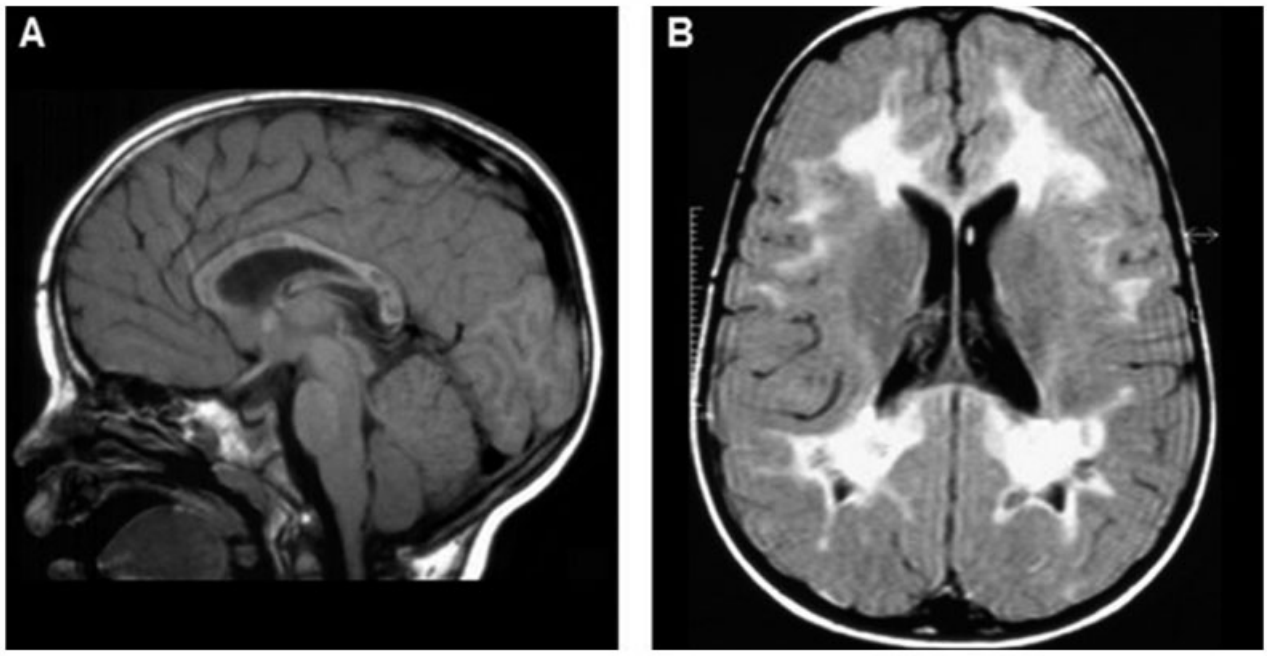

Fig 2. A 2-year-old boy (Patient 2) with mild disease. (A) Sagittal T1-weighted spin-echo and (B) axial fluid-attenuated inversion recovery (FLAIR) images show confluent, bilateral T2 hyperintense white matter lesions in the centrum semiovale with relative sparing of the peri-Rolandic regions, and in the anterior and posterior corona radiata across the corpus callosum, extending to the subcortical white matter but not involving the U-fibers selectively. Multiple foci of cavitation are best seen on the sagittal view within the white matter lesions, in this case in the corpus callosum (A) and in the parietal white matter (B).

riod, whereas those in the posterior regions began to coalesce. In all other patients, the latest MRI showed diffuse white matter abnormalities involving virtually the entire cerebral hemispheres, particularly the corpus callosum. Progressive parenchymal volume loss without collapse of the ventricles was also present. Involvement of basal ganglia (Patient 1), or thalami (as the predominant feature in Patient 3), occurred very late in the course of the illness, in the most severely affected patients (Patients 1 and 3). In five patients, the posterior limb of the internal capsule also was involved. Cerebellar peduncles and cerebellar white matter were affected in Patients 1, 3, and 9 (Fig 3A,B). Brainstem lesions, which emerged in various locations and rarely disappeared with time, included the tracts of substantia nigra, periaqueductal gray, pontine pyramidal tracts, central tegmental tracts, and the central part of the medulla. Small foci of enhancement were found within newly affected white matter, which varied on subsequent studies (see Fig 3E,F). The more prominent the contrast enhancement, the larger the area of involvement and more severe the cystic degeneration that followed. Spinal cord involvement was seen in four patients. In some, this appeared to be an extension of brainstem lesions, but in others holocord signal abnormalities and cystic changes were concurrent or even predominant manifestations as in Patient 17 (see Fig 3G).

Disease Severity and Temporal Evolution

Disease severity could be mild, severe, or variable; some patients regressed rapidly, whereas others were relatively stable over a 3-year period.

MILD BRAIN INVOLVEMENT. Patients 2 (see Fig 2), 4, and 5 had years of relative clinical stability, largely sparing U-fibers, and more limited cystic degeneration.

Clinical Features. Patient 2, a sibling of Patient 1, was normal except for slightly delayed speech until 2 years of age, when he developed a low-grade fever and refused to walk but improved with ibuprofen. When examined at 5.5 years of age, he was neurologically stable with slightly infantile behavior, but normal speech and gait. Head growth followed the 50th centile but his height and weight were at the 10th centile.

Magnetic Resonance Imaging Features. Illustrated in Figure 2 is the MRI of Patient 2 at 2 years 3 months showing extensive signal abnormality with some cystic degeneration of the corpus callosum and of the cerebral hemispheric white matter, with sparing of the U-fibers as seen in pathological section of Patient 12 shown in Figure 5. Within the brainstem, the central tegmental tracts were involved. At 3 years 6 months, there was minimal improvement. The cerebral white matter ab-

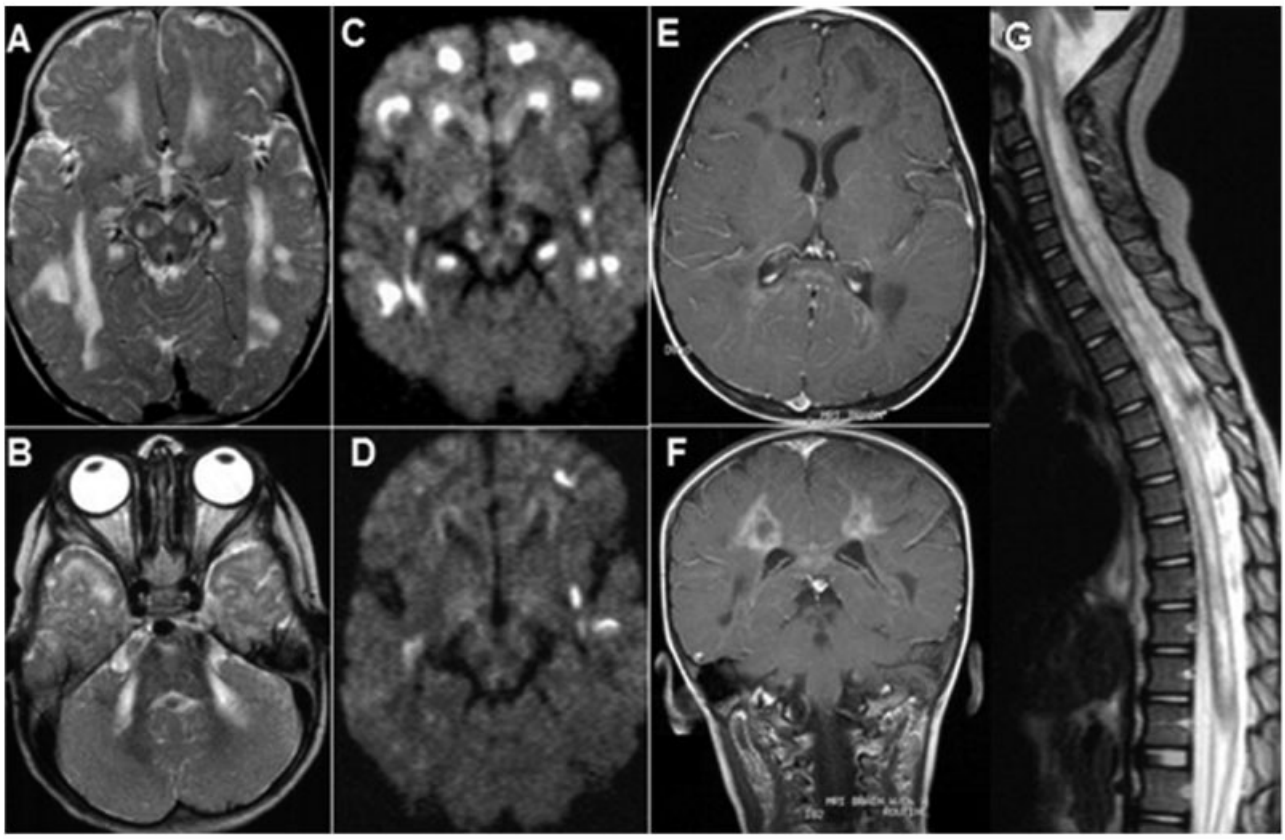

Fig 3. (A, B) Scans for a 16-month old boy (Patient 9) presenting with acute irritability and limping. Magnetic resonance imaging (MRI) shows cerebellar and brainstem lesions in addition to characteristic supratentorial white matter involvement. The pattern of involvement strongly suggests extension along axonal fiber tracts, accounting for the bilateral and nearly symmetric T2 hyperintensity in the cerebral peduncles, pons, middle and inferior cerebellar peduncles, and cervicomedullary junction. (C) Same patient, diffusion-weighted images (DWI) show that many lesions are hyperintense, indicating cytotoxic edema, likely reflecting acute demyelination. (D) Follow-up scan for same patient 6 months later shows resolution of many of these DWI hyperintense lesions whereas appearance of a few new lesions indicate a relapsing course. (E) Axial and (F) coronal postcontrast T1-weighted images for Patient 6 show that a portion of the white matter lesions (eg, parietal periventricular white matter, splenium of the corpus callosum, and minimally genu of the corpus callosum) enhance with GdDTPA. (G) Patient 17, sagittal T2-weighted fast spin-echo image of the spine shows extensive spinal cord disease in addition to characteristic brain involvement with cavitary leukoencephalopathy. In this case, there is holocord involvement with cavitation showing multilocular areas of T2 hyperintensity.

normalities were less extensive, U-fibers remained spared, and the cysts were smaller. The brainstem involvement was, at most, subtle. A follow-up MRI at 5.5 years showed minimal improvement of white matter changes but the cysts remained unchanged.

SEVERE BRAIN INVOLVEMENT. Patients 1 (Fig 4) and 3 had the most diffuse cystic degeneration affecting basal ganglia, thalamus, internal capsule, brainstem, cerebellar peduncles, cerebellar white matter, and cervical spinal cord.

Clinical Features. Patient 1 was in good health until 15 months of age, when, 4 days after measles mumps rubella vaccination, she presented with ataxia, irritability, and opisthotonus. She was given one dose of immunoglobulin G intramuscularly. On day 5, she was noted to be stiff, and lumbar puncture (LP) excluded meningitis. On day 8, she had intermittent seizures for over 14 hours treated with phenobarbital. By age 19 months, a gastrostomy was performed. The first MRI available for review was at 2 years of age. From 2 to 5 years, she used a walker, smiled, comprehended simple verbal commands, and spoke in two- to three-word phrases. At 5 years, she had episodes of sweating, irritability, cyanosis, and progressive spasticity. During one such episode, she had a respiratory arrest requiring a tracheostomy. She could still communicate with eye movements. By 6 years of age, she had no spontaneous movements and was in a vegetative state. At 7 years, she worsened clinically, developed pneumonia, and died.

Magnetic Resonance Imaging Features. Results for Patient 1 are shown in Figure 4, with serial MRI scans at ages 3, 5, and 7 years. Initially, there was characteristic

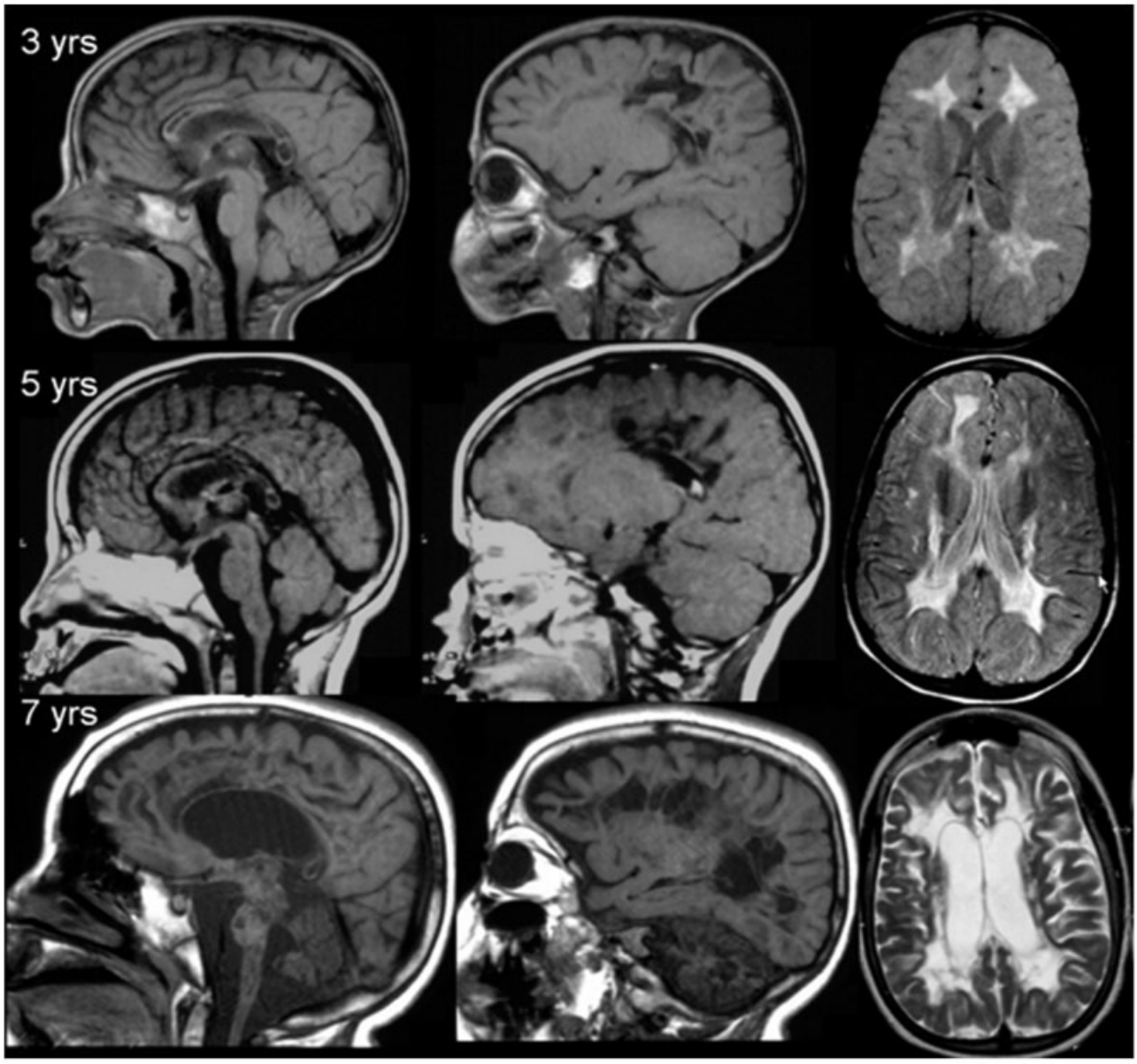

Fig 4. Patient 1 demonstrated progression of disease over a period of 5 years. At age 3 years, sagittal T1-weighted spin-echo and axial proton density images show the common patterns of confluent T2 hyperintense lesions involving the periventricular white matter bilaterally, most notably in the corona radiata and centrum semiovale, extending to the subcortical region, corpus callosum, and posterior limbs of the internal capsules. Note distinct cavitation in the body and splenium of the corpus callosum on sagittal view. At age 5 years, sagittal T1-weighted spin-echo and axial proton density images show that there is more extensive T2 hyperintense signal abnormality, accompanied by interval increase in ventricular size and thinning of the corpus callosum related to parenchymal volume loss. At age 7 years, sagittal T1-weighted spin-echo and axial T2-weighted fast spin-echo images show further progression of disease with increase in signal abnormality also involving the subinsular regions, bilateral thalami, lentiform nuclei (not shown), and brainstem, cerebellum, and upper cervical cord. Note progressive, diffuse parenchymal volume loss and marked thinning of the corpus callosum.

leukoencephalopathy including cavitary lesions in the corpus callosum. Over the next 5 years, there is progressive and profound increase in the extent of signal abnormality that also involves the deep gray matter, brainstem, and upper cervical cord, accompanied by progressive, diffuse parenchymal, and callosal volume loss.

RAPID PROGRESSION. Rapid progression was seen in Patient 5 over a period of 6 months (images not shown).

Clinical Features. Patient 5 was healthy until age 3.5 years, when he developed nasal speech, dysarthria, mild truncal ataxia, chewing, and swallowing difficulties with

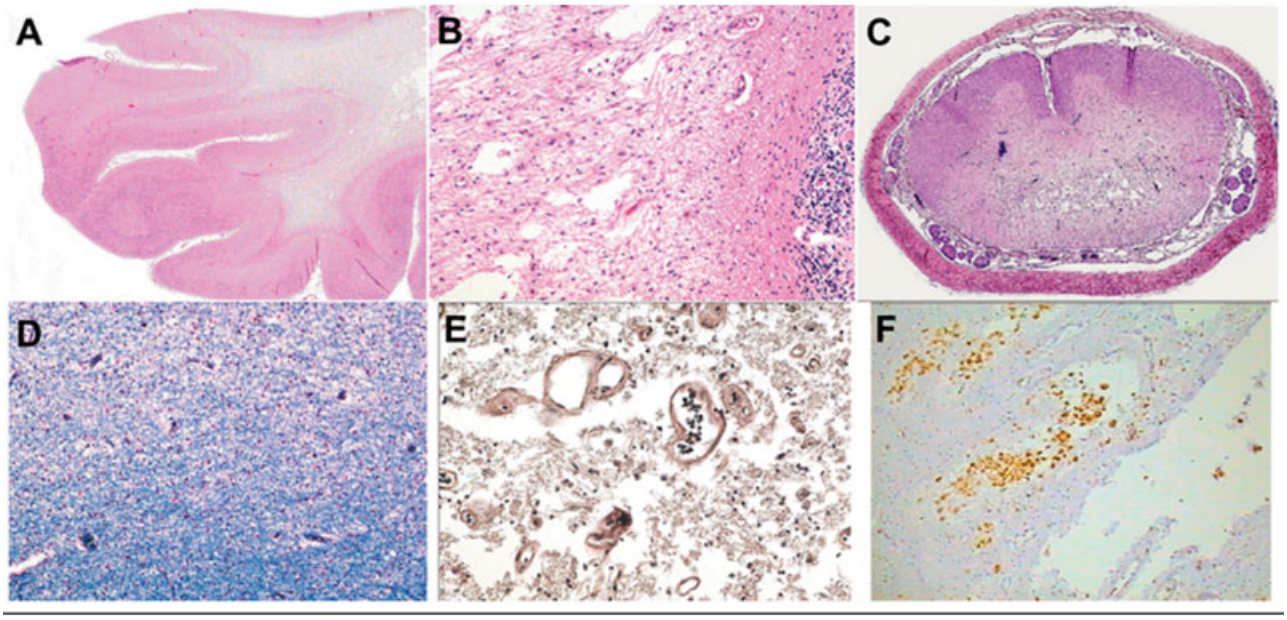

Fig 5. (A–C) hematoxylin and eosin stainings. (A) Brain slice micrograph obtained from autopsy of Patient 12: the cortex and subcortical arcuate fibers are unremarkable, but the deep white matter is pale and shows cystic changes in deeper regions to the far right. (B) In cerebellum of Patient 12, the internal granular layer and myelin immediately adjacent to it is preserved, but there is marked tissue loss with cysts. (C) Spinal cord in Patient 8 shows marked pallor and small cysts in the posterior columns. Bilateral noncystic pallor consistent with secondary tract ("Wallerian") degeneration is present in the spinal cord. (D) Myelin staining in Patient 8 of centrum semiovale with Luxol fast blue shows normal areas (bottom) and early pallor with loosening of the neuropil (top). (E) Bielchowsky stain in cortex of Patient 8 shows axonal disruption in moderately involved areas. (F) In brain of Patient 12, there is no inflammation, but there are some clusters of foamy macrophages within the cavities shown by use of CD68 antibody.

nasal reflux and facial diplegia. There was no evidence of metabolic or infectious involvement, and CSF was normal. He was treated for possible acute disseminated encephalomyelitis (ADEM) with methylprednisolone and then with oral prednisone that was tapered over 1 month. Despite some recovery after steroids, at 3 years 7 months he developed bilateral upper extremity weakness with diffuse hyperreflexia and bilateral Babinski responses. Repeated testing for infections was negative, but CSF showed lactic acidosis. He was treated again with steroids, which was tapered over the next 2 months. At 4 years, he again became dysarthric, had swallowing difficulties, was unable to walk, and had a weak grasp. Because both MRS and CSF showed increased lactate levels, a mt disease was suspected, and higher doses of steroids (IVIG) and carnitine were given. Later DCA was added. He slowly recovered but had residual spasticity, dysarthria, and ataxia. He remained in this state for over 1 year, without further acute episodes. Brain biopsy is described under pathology.

Magnetic Resonance Imaging Features. In five patients between ages 3.5 years and 4 years, initial MRIs showed multifocal lesions in the deep cerebral white matter. In 6 months, the cystic lesions became progressively larger and more confluent, resulting in a diffuse cavitating leukoencephalopathy pattern involving almost all of the cerebral hemispheric white matter and corpus callosum, extending to C2 to 3 levels. Changing foci of contrast enhancement were seen within the cerebral white matter and corpus callosum.

Pathology. Brain biopsy (Patient 5) and autopsies were performed (Patients 8, 12, and 13; Fig 5). Despite the extensive brain involvement, brain weights were within normal limits for age in these three patients. There were no developmental abnormalities, and the brains had not collapsed because of the cystic degeneration. The cerebral and cerebellar cortical white matter and portions of the corpus callosum were maximally involved. Macroscopically, some areas of the cerebral white matter were soft and had cavitations up to 1cm in diameter. Microscopically, the lesions were confined to the white matter, whereas cerebral and cerebellar gray matter was spared. The lesions were often multifocal and unevenly distributed, and the more peripheral cysts spared the digitate white matter, including the U-fibers. The cysts were well demarcated from adjacent normal white matter. Histologically, early lesions consisted of pallor and loosening of the neuropil, with some loss of oligodendrocytes. In the more advanced lesions, the neuropil became even looser with loss of the normal myelin staining. Oligodendrocytes disappeared with axonal disruption and eventually cavitation

occurred. There was no spongiosis. Reactive gliosis if present was very mild and there was no inflammation. Occasionally clusters of foamy macrophages could be seen within the cavities. In the brain biopsy of Patient 5, electron microscopy (EM) showed glial hyperplasia and macrophages containing myelin lamellae, microscopic evidence of myelin loss, reduced oligodendroglia, macrophages, and axonal disruption. No vasculopathy was identified.

Discussion

Clinical and Laboratory Findings

The essential features of progressive cavitatory leukoencephalopathy (PCL) are irregular asymmetric patchy areas of white matter abnormality that evolve to develop cystic degeneration. The cystic changes involve especially the corpus callosum, cerebral and cerebellar white matter, and spinal cord, with varying degrees of contrast enhancement. In terminal stages, the cystic degeneration involves all of the white matter of the cortical regions, and spinal cord, with relative sparing of the U-fibers and gray matter. In its initial stages, differentiation from acute infectious, postinfectious, or immunological conditions may be difficult, because MRI shows only multiple isolated contrast enhancing lesions within the abnormal cerebral or cerebellar white matter. An important finding is the increase of lactate in blood, CSF, or in affected brain regions on MRS. Peripheral neuropathy in some may have been aggravated by DCA treatment. Seizures were rare and EEG was often diffusely slow without spikes.

In some, the acute phase of PCL has features of severe encephalopathy, with irritability and opisthotonic posturing, but without increased intracranial pressure or CSF evidence of infections. The occasional elevation of lactate, although not yet attributable to a known mt defect, could be related to mt dysfunction or toxicity or possibly inflammation,[6,7] but the finding of increased levels of lactate in CSF and blood in some subjects suggests a primary metabolic cause for the abnormal MRS lactate levels. The associated contrast enhancement indicates altered vascular permeability, but the lack of perivascular lymphocytic infiltration argues against an infectious or inflammatory cause, or immunological response to a primary insult. New silent lesions must occur between acute episodes because sequential neuroimaging studies demonstrate new areas of contrast enhancement and additional cavities. During periods of remission patients recover some skills, although not to previous levels. Neither Patient 3, at age 13 years, nor Patient 2, at age 6 years, showed newer lesions on MRI. Although Patient 3 had very little white matter left to be affected, in Patient 2, with a milder form of PCL, the disease may have become static. One could speculate that there is an age-related toxic effect as in some mt-based organic acidurias, for example, glutaric aciduria.[8]

Pathophysiology and Differential Diagnosis

Lesions in brain and spinal cord white matter are characterized by myelin loss in the younger lesions, without inflammation. Moderate and severely affected regions with cystic degeneration and loss of axonal integrity coexist. Specific tracts showing vulnerability include the corticospinal tracts, interhemispheric tracts of the corpus callosum, central tegmental tracts, cerebellar peduncles, and spinal cord.

Progressive clinical deterioration with cystic changes on MRI are seen in various disorders including mt defects causing Leigh's syndrome,[9] MLC1,[1,2] microcephalic leukoencephalopathy with cysts,[3] late stages of Alexander's disease,[10] and infections processes.[11] In our patients, the episodic nature of acute deteriorations, without evidence of preceding brain infections or obvious metabolic stress, differs from the chronic progressive course seen in the above conditions, with the exception of Leigh's disease, in which episodic deterioration also is common. The episodic clinical regression, increased lactate, and related biochemical abnormalities in several patients suggest a mt disorder. Although no known mt DNA mutations or deletions were detected, they constitute less than 10% of pediatric mt diseases.

The differential diagnosis of PCL includes the following. (1) ADEM, in which multiple and asymmetric lesions involve both gray and white matter,[12] sometimes with contrast enhancement.[13,14] However, the recurrent acute clinical presentation with cystic degeneration is not a feature of ADEM, although the initial episode may suggest this diagnosis.

(2) Autosomal dominant acute necrotizing encephalopathy (ADANE) is a disorder that maps to 2q12-13 and resembles the acute encephalopathic picture of PCL.[15,16] However, in ADANE the thalamus is primarily involved, white matter changes are especially prominent in the brainstem, and an increased CSF protein is a consistent finding during the acute phase of the disease. In one patient with ADANE, muscle biopsy showed pleomorphic mt with cytoplasmic vacuoles, and muscle mt had loose coupling of oxidative phosphorylation. ADANE may be fatal or patients can survive with developmental delay and neurological deficits. The episodes are accompanied by cavitation of the thalami and white matter. The predominant thalamic involvement on MRI, histological evidence of involvement of both gray and white matter, and consistently increased CSF protein differ from PCL.

(3) Hemophagocytic lymphohistiocytosis (HLHs) is a devastating and etiologically heterogenous neurological disorder. Primary HLH is caused by an autosomal recessive disorder of immune regulation, whereas secondary HLH is associated with infectious agents such as Epstein–Barr virus.[17] In primary and secondary HLH, there is acute neurological deterioration with abnormal white matter and cystic degeneration. The familial dis-

ease is caused by mutations in genes critical in the perforin/granzyme pathway used by cytotoxic lymphocytes to eliminate virus-infected or transformed cells.[18] Patients with HLH show lack of intracellular perforin in all cytotoxic cell types (natural killer cells, $CD8^+$ T cells, and $CD56^+$ T cells), caused by mutations in the perforin gene, whereas perforin mutation carriers have abnormal perforin-staining patterns. In addition to perforin 1 defects, mutations in syntaxin 11 and UNC13D genes also result in familial HLH.[19,20] In contrast, nonfamilial, virus-associated HLH has depressed numbers of natural killer cells but markedly increased proportions of $CD8^+$ T cells and normal perforin expression.[21] The acute phase consists of an infectious prodrome with fever, organomegaly, cytopenias, and severe neurological deficits. Brain pathology, however, differs from PCL in abundant meningeal infiltration by lymphocytes and macrophages. Advanced cases show perivascular or diffuse infiltration in brain tissue, as well as multifocal necrosis with prominent astrogliosis.[22] These clinical and pathological differences readily distinguish HLH from PCL.

(4) Mitochondrial dysfunction is suggested in our patients by increased lactate in blood, CSF, and brain MRS. Abnormal urine organic acids also suggested mt dysfunction but were variable. Although increased lactate levels may be detected in brain MRS at the edge of a lesion where there is myelin breakdown as in ALD,[7] the association of hyperlactacidemia and abnormal urinary organic acids suggests a diffuse disturbance in mt function. Muscle and brain biopsies showed no abnormalities in mt morphology, except for Patient 4. None had documented hearing loss or cardiac involvement common to mt disorders. Peripheral neuropathy was evident in two older children, yet this may be confounded by their treatment with DCA, which is known to cause peripheral neuropathy. Contrary to most primary mt dysfunctions, our patients had no accompanying gray matter involvement and no detectable favorable response to treatment with "cocktails" of vitamins, cofactors, or DCA therapy (although such therapy was not provided in a consistent manner). The absence of an identifiable and consistent abnormality in the mt respiratory chain or in mt DNA, however, does not exclude involvement of a nuclear encoded mt gene. Alternatively, mt dysfunction could be secondary to endogenous toxins.

Our report identifies a subset of children with a uniform clinical, pathological, and neuroradiological picture suggestive of a distinct nosologic entity. Although this entity could be causatively heterogenous, the familial occurrence and consanguinity suggest autosomal recessive inheritance. We are investigating the possibility of mutations in nuclear encoded genes affecting mt function and energy metabolism, or in genes controlling axonal myelin interaction as the cause of this disorder.

References

1. van der Knaap MS, Barth PG, Stroink H, et al. Leukoencephalopathy with swelling and a discrepantly mild clinical course in eight children. Ann Neurol 1995;37:324–334.
2. Gorospe JR, Singhal BS, Kainu T, et al. Indian Agarwal megalencephalic leukodystrophy with cysts is caused by a common MLC1 mutation. Neurology 2004;23;62:878–882.
3. Henneke M, Preuss N, Engelbrecht V, et al. Cystic leukoencephalopathy without megalencephaly: a distinct disease entity in 15 children. Neurology 2005;64:1411–1416.
4. Canavan MM. Schilders encephalitis perioxolis diffusa. Neurology 1931;15:299–308.
5. Golay X, Gillen J, van Zijl PC, Barker PB. Scan time reduction in proton magnetic resonance spectroscopic imaging of the human brain. Magn Reson Med 2002;47:384–387.
6. Tzika AA, Ball WS Jr, Vigneron DB, et al. Childhood adrenoleukodystrophy: assessment with proton MR spectroscopy. Radiology 1993;189:467–480.
7. Pouwels PJ, Kruse B, Korenke GC, et al. Quantitative proton magnetic resonance spectroscopy of childhood adrenoleukodystrophy. Neuropediatrics 1998;29:254–264.
8. Strauss KA, Puffenberger EG, Robinson DL, Morton DH. Type I glutaric aciduria, part 1: natural history of 77 patients. Am J Med Genet C Semin Med Genet 2003;121:38–52.
9. Farina L, Chiapparini L, Uziel G, et al. MR findings in Leigh syndrome with COX deficiency and SURF-1 mutations. AJNR Am J Neuroradiol 2002;23:1095–1100.
10. Johnson AB, Brenner M. Alexander's disease: clinical, pathologic, and genetic features. J Child Neurol 2003;18:625–632.
11. De Recondo A, Guichard JP. Neurological picture. Acute disseminated encephalomyelitis presenting as multiple cystic lesions. J Neurol Neurosurg Psychiatry 1997;63:15.
12. Hynson JL, Kornberg AJ, Coleman LT, et al. Clinical and neuroradiologic features of acute disseminated encephalomyelitis in children. Neurology 2001;56:1308–1312.
13. Bizzi A, Ulug AM, Crawford TO, et al. Quantitative proton MR spectroscopic imaging in acute disseminated encephalomyelitis. AJNR Am J Neuroradiol 2001;22:1125–1130.
14. Lim KE, Hsu YY, Hsu WC, Chan CY. Multiple complete ring-shaped enhanced MRI lesions in acute disseminated encephalomyelitis. Clin Imaging 2003;27:281–284.
15. Mizuguchi M. Acute necrotizing encephalopathy of childhood: a novel form of acute encephalopathy prevalent in Japan and Taiwan. Brain Dev 1997;19:81–92.
16. Neilson DE, Feiler HS, Wilhelmsen KC, et al. Autosomal dominant acute necrotizing encephalopathy maps to 2q12.1-2q13. Ann Neurol 2004;55:291–294.
17. Loy TS, Diaz-Arias AA, Perry MC. Familial erythrophagocytic lymphohistiocytosis. Semin Oncol 1991;18:34–38.
18. Stepp SE, Dufourcq-Lagelouse R, Le Deist F, et al. Perforin gene defects in familial hemophagocytic lymphohistiocytosis. Science 1999;286:1957–1959.
19. Feldmann J, Callebaut I, Raposo G, et al. Munc13–4 is essential for cytolytic granules fusion and is mutated in a form of familial hemophagocytic lymphohistiocytosis (FHL3). Cell 2003;115:461–473.
20. zur Stadt U, Schmidt S, Kasper B, et al. Linkage of familial hemophagocytic lymphohistiocytosis (FHL) type-4 to chromosome 6q24 and identification of mutations in syntaxin 11. Hum Mol Genet 2005;14:827–834.
21. Kogawa K, Lee SM, Villanueva J, et al. Perforin expression in cytotoxic lymphocytes from patients with hemophagocytic lymphohistiocytosis and their family members. Blood 2002;99:61–66.
22. Henter JI, Nennesmo I. Neuropathologic findings and neurologic symptoms in twenty-three children with hemophagocytic lymphohistiocytosis. J Pediatr 1997;130:358–365.